academicJournals

Vol. 7(40), pp. 4828-4834, 4 October, 2013
DOI: 10.5897/AJMR2013.5926
ISSN 1996-0808 ©2013 Academic Journals
http://www.academicjournals.org/AJMR

African Journal of Microbiology Research

Full Length Research Paper

Alteration of BHK-21 cells proteome after foot-and-mouth disease virus infection

Keshan Zhang, Guodong Lu, Yongjie Liu, Hanjin Kong, Youjun Shang and Xiangtao Liu*

State Key Laboratory of Veterinary Etiological Biology, National Foot and Mouth Disease Reference Laboratory, Lanzhou Veterinary Research Institute, Chinese Academy of Agricultural Sciences, Lanzhou 730046, China.

Accepted 6 September, 2013

Foot-and-mouth disease is a highly contagious viral illness of wild and domestic cloven-hoofed animals. The complex relationship of FMDV and with the host cells leads to its replication and spread. BHK-21 cell line is an *in vitro* model for FMDV infection and is commonly used for viral seed preparation. In order to better understand the molecular basis of this relationship, a proteomics study on baby hamster kidney cells infected with FMDV was performed. The differential proteomes of BHK-21 cells, with and without BHK-21 infection, were analyzed with two-dimensional gel electrophoresis (2-DE) followed by MALDI-TOF/TOF identification. Mass spectrometry identified 30 altered protein spots (19 up-regulated, 9 down-regulated and 2 viral protein spots), which included metabolic processes proteins, cytoskeletal proteins, microfilament-associated proteins, stress response proteins and FMD viral proteins. Western blot analysis further confirmed the differential expression of protein NME-2 in the proteomic profiles. Subcellular location demonstrated NME2 protein was distributed in BHK-21 cell cytoplasm and nucleolus. Thus, this work provides useful proteinrelated informations to further understand the underlying pathogenesis of FMDV infection.

Key words: Foot-and-mouth disease virus, BHK-21 cells, comparative proteomics, 2-DE, NME2.

INTRODUCTION

Foot and mouth disease virus (FMDV) causes a highly infectious disease of cloven-hoofed animals that has significant global socioeconomic impact (Schley et al., 2012). Although FMD does not result to high mortality in adult animals, the disease has negative effects, including decrease in milk production, weight loss and loss of draught power, resulting in a loss in productivity for a considerable time (Wang et al., 2012). However, mortality can be high in young cloven-hoofed animals, where the virus can affect the heart. In countries where FMD is endemic the disease results in enormous losses and it is ranked in the top ten livestock diseases for cattle and pigs in terms of impact on the poor globally. FMDV belongs to the *Picornaviridae* family and has single-stranded, positive-sense RNA, with seven serotypes and its genome has one large open reading frame (ORF), which encodes a precursor protein (Bachrach, 1968; Leforban, 1999; Martinez-Salas et al., 2008). After processing by proteases, the precursor protein is split into single proteins, including four structural proteins, that is, VP1, VP2,VP3 and VP4, and eight nonstructural proteins, that is, L^{pro}, 2A, 2B, 2C, 3A, 3B, $3C^{pro}$ and $3D^{pol}$ (Rueckert, 1996). The BHK-21 cell line provides ideal cells for researching the infectious and pathogenic mechanism of

*Corresponding author. E-mail: hnxiangtao@hotmail.com. Tel: +86 931 8343307. Fax: +86 931 8342052.

Abbreviations: CAN, acetonitrile; **BHK,** baby hamster kidney; **CPE,** cytopathic effect; **ER,** endoplasmic reticulum; **FMDV,** foot and mouth disease virus; hpi, hours pos-tinfection; **MS,** mass spectrometry; **TFA,** trifluoroacetic acid.

FMDV (Huang et al., 2011; Mitev and Tekerlekov, 1973; Ubertini et al., 1967).

Proteomic technology that couple two-dimensional electrophoresis (2-DE) and mass spectrometry (MS) are widely used (Aebersold and Mann, 2003; Blackstock and Weir, 1999), it is a powerful tool for providing insights into pathogenesis, diseases biomarkers, and the prevention of disease (Hanash, 2003; Misek et al., 2011; Wright Jr and Semmes, 2003). Proteomic alteration in infected host cells have been studied in major pathogenic animal disease viruses, including classical swine fever virus (PK-15 cells were used) (Sun et al., 2008), African swine fever virus (Vero cells were used) (Alfonso et al., 2004), porcine reproductive and respiratory syndrome virus (pulmonary alveolar macrophage were used) (Zhang et al., 2009), infectious bursal disease virus (chicken embryo fibroblasts were used) (Zheng et al., 2008) and rabies virus (BHK-21 cells were used) (Zandi et al., 2009).

In the present study, a baby hamster kidney (BHK) cell line (BHK-21) was infected with FMDV serotype Asia1 and the proteome pattern of the cell was investigated 12 h post infection. This simple mammalian cell infection model was selected to analyze the direct effect of FMDV on cell protein machinery free from influences of external stimuli. A total of 30 differentially expressed protein spots were identified. We found that viral proteins, host cell cytoskeletal proteins, microfilament-associated proteins, stress response proteins were the main proteins with significant altered expression profile. Further analysis of these data provides clues to understanding the replication and pathogenesis of FMDV and the virus-host interactions.

MATERIALS AND METHODS

Cell culture, virus inoculation

FMDV serotype Asia1 was provided by the National Foot-and-Mouth Disease Reference Laboratory in Lanzhou, China. BHK-21 cells were cultured in modified Eagle's medium (MEM, HyClone) supplemented with 10% fetal bovine serum, 100 U/mL penicillin G and 100 mg/mL Na streptomycin sulfate at 37°C in 5% CO_2 until they formed a monolayer. After washing three times with PBS (pH 7.4), the cells were inoculated with FMDV serotype Asia1. Uninfected cells were incubated in MEM as a mock-infected control. Fluorescence quantitative RT-PCR was used to valuate FMDV reproduction interval two hours.

Protein extraction, 2-DE gel staining and image analysis

The infected and uninfected cells were mechanically scraped and collected into centrifuge tubes 12 hpi. After three cycles of washing with ice-cold PBS (pH 7.4) and centrifugation (8000 x*g* for 5 min), harvested cells were lysed with lysis buffer containing 7 M urea, 2 M thiourea 4% CHAPS, 20 mM Tris, 50 mM DTT, 0.5% IPG buffer and 1 mM FMSF at a volume ratio of 1:20. After 2 h on ice, DNase and RNase were added to the mixture at final concentrations of 20 U/mL and 0.25 mg/mL, respectively, and nucleic acids were degraded on ice for 1 h. After centrifugation at 16000 x*g* for 20 min at 4°C, the supernatants were collected and the protein concentration was determined using a Quant kit (Bio-Rad).

2-DE using 7 cm IPG strips at nonlinear pH 3-10 (Bio-Rad) in the first dimension isoelectric focusing (IEF) were performed. The IPG strips were rehydrated with 150 µL of rehydration buffer (8 M urea, 4% CHAPS, 50 mM DTT, 0.2% IPG buffer pH 3~10 NL, and trace amount of bromophenol blue) containing 100 µg of protein samples, before staining with Coomassie brilliant blue. Active rehydration was achieved by applying 50 V for 12 h. IEF was carried out at 18°C in a Protean IEF cell (Bio-Rad), where the current was limited to 50 mA/strip with the following voltage program: 500 V linear for 30 min, 1000 V rapid for 30 min, 4000 V linear for 3 h, then 4000 V constant for a total of 20 000 Vh. After IEF, the IPG strips were equilibrated by soaking for 15 min in 50 mM Tris-HCl, pH 8.8, 6 M urea, 2% SDS, 30% glycerol, 2% (w/v) DTT, and a trace of bromophenol blue. This was followed by another 15 min in the same solution, which contained 2.5% (w/v) iodoacetamide instead of DTT. The second-dimensional separation was performed using 12% homogeneous SDS polyacrylamide gel. Electrophoresis was carried out at a constant current of 80 V/gel for 5 min, followed by 200 V/gel, until the dye reached the bottom of the gel.

The gels were stained with Coomassie brilliant blue and scanned at a resolution of 500 dots/inch using a scanner (GS-800 Calibrated Densitometer). Spot detection, matching and quantitative intensity analysis were performed using the PDQuest 2-D analysis program (Bio-Rad). A relative comparison of intensity abundance was performed between FMDV-infected and mock-infected groups (three replicate samples for each group) using the Student's *t*-test. Infected /uninfected expression intensity ratios higher than 2.0 ($p \leq 0.05$) or less than 0.5 ($p \leq 0.05$) were set used as threshold values to detect significant differences.

Enzymatic digestion, MALDI-TOF/TOF MS and database search

Significant differential protein spots were excised manually from Coomassie-stained gels and washed with 100 µL 50% v/v acetonitrile (ACN) in 25 mM ammonium bicarbonate for 1 h. After dehydration with 100% v/v ACN for 20 min, the gel pieces were dried thoroughly with a speedVac concentrator (Thermo Savant, U.S.A) for 30 min. The dried gel particles were rehydrated for 45 min at 4°C with 2 µL trypsin (Promega, Madison, WI) in 25 mM ammonium bicarbonate and then incubated for 12 h at 37°C. The resulting peptides were extracted three times using 8 µL aliquots of 5% trifluoroacetic acid (TFA) in 50% ACN for 1 h at 37°C and dried by vacuum centrifugation.

The peptide mixtures were redissolved in 0.8 uL of matrix solution (α-cyano-4-hydroxycinnamic acid (Sigma) in 0.1% TFA and 50% ACN) and then spotted onto a MALDI plate. Samples were allowed to air-dry and analyzed using a 4700 MALDI-TOF/TOF Proteomics Analyzer (Applied Biosystems, Foster City, CA). Trypsin-digested peptides of myoglobin were added to the six calibration spots on the MALDI plate to calibrate the mass instrument in the internal calibration mode. The UV laser was operated at a 200-Hz repetition rate with a wavelength of 355 nm. The accelerated voltage was operated at 20 kV. All acquired spectra of samples were processed using the 4700 ExploreTM program (Applied Biosystems) in the default mode. Parent mass peaks with a mass range of 700-3200 Da and a minimum signal to noise ratio of 20 were selected for tandem TOF/TOF analysis.

Combined MS and MS/MS spectra were submitted to MASCOT (Version 2.1, Matrix Science, London, UK) using the GPS explorer program (Version 3.6, Applied Biosystems) and searched using the following parameters in the National Center for Biotechnology Information non-redundant (NCBInr) database (release date, March 18, 2006): taxonomy of bony vertebrates or viruses, trypsin digest with one missing cleavage, no fixed modifications, MS tolerance of 0.2 Da, MS/MS tolerance of 0.6 Da, and possible oxidation of methionine. Known contaminant ions (human keratin and tryptic autodigest peptides) were excluded. A total of 4,736,044 sequences

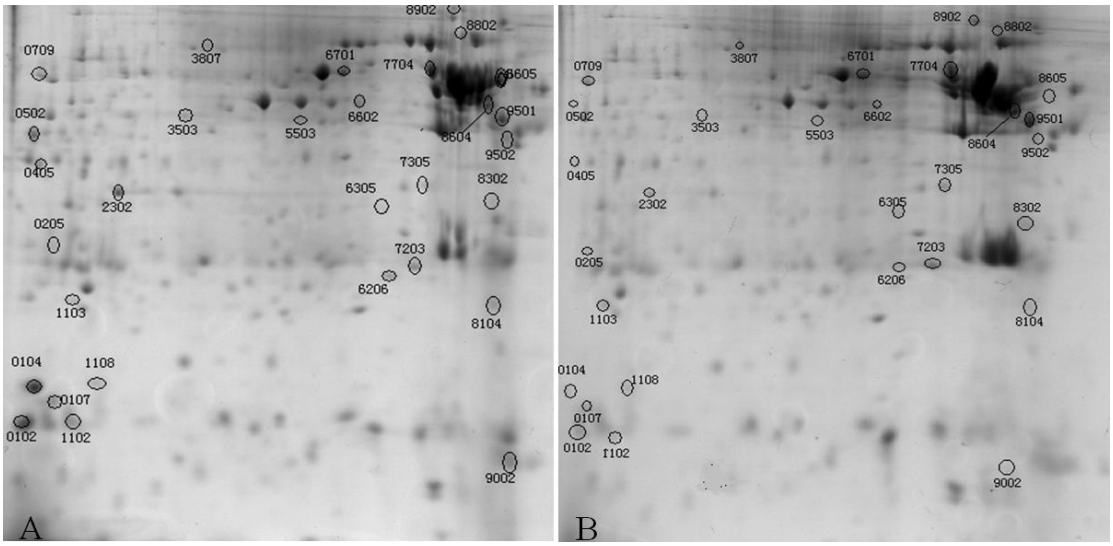

Figure 1. 2-DE analysis of FMDV-infected BHK-21 cells at 12 hpi. Circles show the protein spots from which the proteins were isolated. (A) FMDV infected cells; (B) non-infected cells

and 1,634,373,987 residues were actually searched in the database. MASCOT protein scores (based on combined MS and MS/MS spectra) > 72 were considered statistically significant ($p \leq 0.05$). We accepted individual MS/MS spectra with a statistically significant (confidence interval ≥ 95%) ion score (based on MS/MS spectra). To eliminate the redundancy of proteins that appeared in the database with different names and accession numbers, we singled out a single protein member belonging to the species *Gallus* or that with the highest protein score (top rank) from a multiprotein family.

Data analysis

Protein classification was conducted using Gene Ontology Annotation (GOA; http://www.ebi.ac.uk/goa/), according to molecular functions and biological processes. The subcellular location of different proteins was predicated with PSORT (http://psort.hgc.jp/).

Western blot analysis

A total of 50 mg proteins from FMDV-infected and mock-infected BHK-21 cells at 12 h post infection (hpi) were mixed with an equal volume of SDS-PAGE loading buffer and boiling for 5 min. After separation using 12% sodium dodecyl sulfate polyacrylamide gels, proteins were electro-transformed onto PVDF membranes and blocked nonspecifically using 1% BSA in 0.01 mol/L PBS, pH 7.4, for 2 h at room temperature. Membranes were then incubated successively for 2 h at ambient temperature with mouse monoclonal antibodies to NME2 (Abcam, Cambridge, U.K.). After three 15 min washes with PBST, the membranes were further incubated with rabbit anti-mouse IgG conjugated with horseradish peroxidase (Sigma, St. Louis, MO) (1:5000 dilution in 1% BSA in 0.01 mol/L PBS, pH 7.4) at room temperature for 2 h. Reactive protein stripes were visualized using Super Signal West Pico Chemiluminescence Substrate (Pierce Biotechnology, Inc., Rockford, IL) after three times washes with PBST. Equal protein loading was confirmed by exposure of the membranes to anti β-actin antibody.

Subcellular localization of NME2 in BHK-21 cells

Primers for the NME2 gene were designed based on reference sequences published in GenBank and then synthesized (Takara Co. Ltd). The forward primer sequence was 5′-CCCAAGCTTATGGCCAACCTCGAGCGTACCTT-3′ and the reverse primer sequence was 5′-CGGGATCCCTCATACACCCAGTCATGGGCA-3′. Total RNA from BHK-21 cells was extracted using an RNA Mini Kit (Qiagen, Hilden, Germany), according to the manufacturer's instructions. The NME2 gene was amplified by reverse transcription polymerase chain reaction (RT-PCR) and cloned into the pEGFP-N1 vector (Invitrogen, USA) directionally with the restriction endonucleases *Bam*HI and *Hind*III. The recombinant plasmid was identified by PCR, restriction enzyme digestion analysis, and sequencing.

Empty pEGFP-N1 and recombinant plasmid pEGFP-NME2 were transfected into BHK-21 separately using LipofectamineTM 2000, according to the manufacturer's instructions (Invitrogen, Carlsbad, CA). After transfection for 12 h, cells were washed twice with PBS and fixed with cold acetone/methanol (1:1) for 20 min at -20°C. Cell nuclear staining was performed with 4′,6-diamidino-2-phenylindole (Sigma) for 5 min and washed three time with PBS. Subcellular location of NME2 was observed using a Zeiss LSM510 laser confocal microscope.

RESULTS

All gels provided high resolution separation of proteins, with each detecting over 800 protein spots (Figure 1). On the basis of the average intensity ratios of protein spots, a total of 30 protein spots were identified, including 19 significantly upregulated protein spots (ratio infection/control ≥2, $p \leq 0.05$), 9 significantly downregulated protein spots (ratio infection/control ≤ 0.5, $p \leq 0.05$), and 2 FMDV proteins.

The combined MS and MS/MS analysis with MASCOT database searching successfully identified 30 proteins, including 19 upregulated and 9 downregulated intracellular proteins, and 2 FMDV proteins (Table 1). The cellular proteins identified were involved mainly in five groups, which included morphogenesis, protein synthesis, meta-

Table 1. List of the differentially expressed protein spots in FMDV-infected BHK-21 cells identified by MALDI-TOF or MALDI-TOF/TOF.

Spot no.[a]	Protein name	Abbr.	Accession no.[b]	MW (Da)	pI	Protein score[c]	Sequence coverage[d]
Significantly up-regulated proteins							
5503	beta-actin (aa 27-375)	ACTB	gi|49868	39446	5.78	190	25
3503	gamma-actin	ACTC	gi|809561	42053	5.23	191	28
8605	vimentin	VIM	gi|2078001	51590	4.96	587	56
9502	vimentin	VIM	gi|2078001	51590	4.96	305	48
8802	glucose-regulated protein precursor	GRP78	gi|254540166	68569	5.15	210	29
0205	enoyl-CoA hydratase, mitochondrial precursor	ECHMP	gi|29789289	31853	8.76	118	23
8902	unnamed protein	NP	gi|74228123	97243	5.39	65	12
0502	fructose-bisphosphate aldolase A isoform 2	FBAA2	gi|6671539	39787	8.31	206	34
0405	mitochondrial malate dehydrogenase 2	NAD2	gi|89574115	32113	7.70	81	19
6602	hypothetical protein LOC433182	LOC	gi|70794816	47931	6.63	99	17
0709	ATP synthase	ATPase	gi|148677501	54675	8.24	348	40
0107	Non-metastatic protein2	NME2	gi|154550673	16460	7.77	187	25
0102	Peptidyl isomerase A	PA	gi|6679437	18131	7.74	174	42
1102	Peptidyl isomerase A	PA	gi|6679439	18131	7.74	233	36
0104	cofilin-1	C1	gi|6680924	18776	8.22	170	54
1108	cofilin CRA-b2	CCB2	gi|148704795	19300	7.59	183	40
9002	mCG140959, isoform	mCG1	gi|148692630	17959	4.52	228	21
8302	mCG22236	mCG2	gi|148683218	28993	4.71	88	27
8104	mCG10592, CRA-c	mCG1C	gi|148703873	16581	5.23	108	19
Significantly down-regulated proteins							
1103	peroxiredoxin 1	PXD1	gi|123230137	19669	6.28	141	32
7203	gamma actin	ACTC	gi|123298587	32941	5.15	253	25
7305	Pyruvate dehydrogenase	PDE1	gi|18152793	4387	6.61	117	30
6305	CP isoform 1	CPI1	gi|4826695	29463	6.14	103	46
3807	isoform C	IC	gi|161760667	65508	6.25	101	21
6701	disulfide-isomerase A3	DIA3	gi|112293264	57103	5.78	183	26
9501	vimentin	VIM	gi|2078001	51590	4.96	443	47
8604	vimentin	VIM	gi|2078001	51590	4.96	381	60
7704	Hspd1 protein	Hsp	gi|76779273	59559	8.09	474	39
Viral proteins of FMDV							
2302	nonstructural protein 2C	2C	gi|16902989	36281	7.74	186	21
6206	precursor protein P1	P1	gi|15419535	80620	6.44	202	12

[a]Spot no. is the unique sample spot protein number that refers to the labels in Figure 1. [b]Accession no. is the MASCOT result of MALDI-TOF/TOF searched from the NCBInr database. [c]Protein score (based on combined MS and MS/MS spectra) were from MALDI-TOF/TOF. [d]Sequence coverage (%) is the number of amino acids spanned by the assigned peptides divided by the sequence length.

metabolism and stress response. The proteins were classified according to their biological function (Figure 2A) and subcellular location (Figure 2B). To confirm the dynamic changes in proteins during FMDV infection, we performed a western blot analysis of the NME2, where β-actin was used as an internal control. NME-2 spot number was labelled 0107 in Table 1 and Figure 1. NME2 expression was significantly upregulated at 12 hpi when compared with uninfected cells (Figure 3). This result was consistent with the 2-D PAGE analysis. Subcellular distribution of NME2 indicated that the NME2 protein was distributed in the cytoplasm and nucleolus (Figure 4).

DISCUSSION

Increasing evidence emphasizes comparative proteomics to screen the differentially expressed proteins associated with host cellular pathophysiological processes of virus infection (Maxwell and Frappier, 2007). BHK-21 cells was

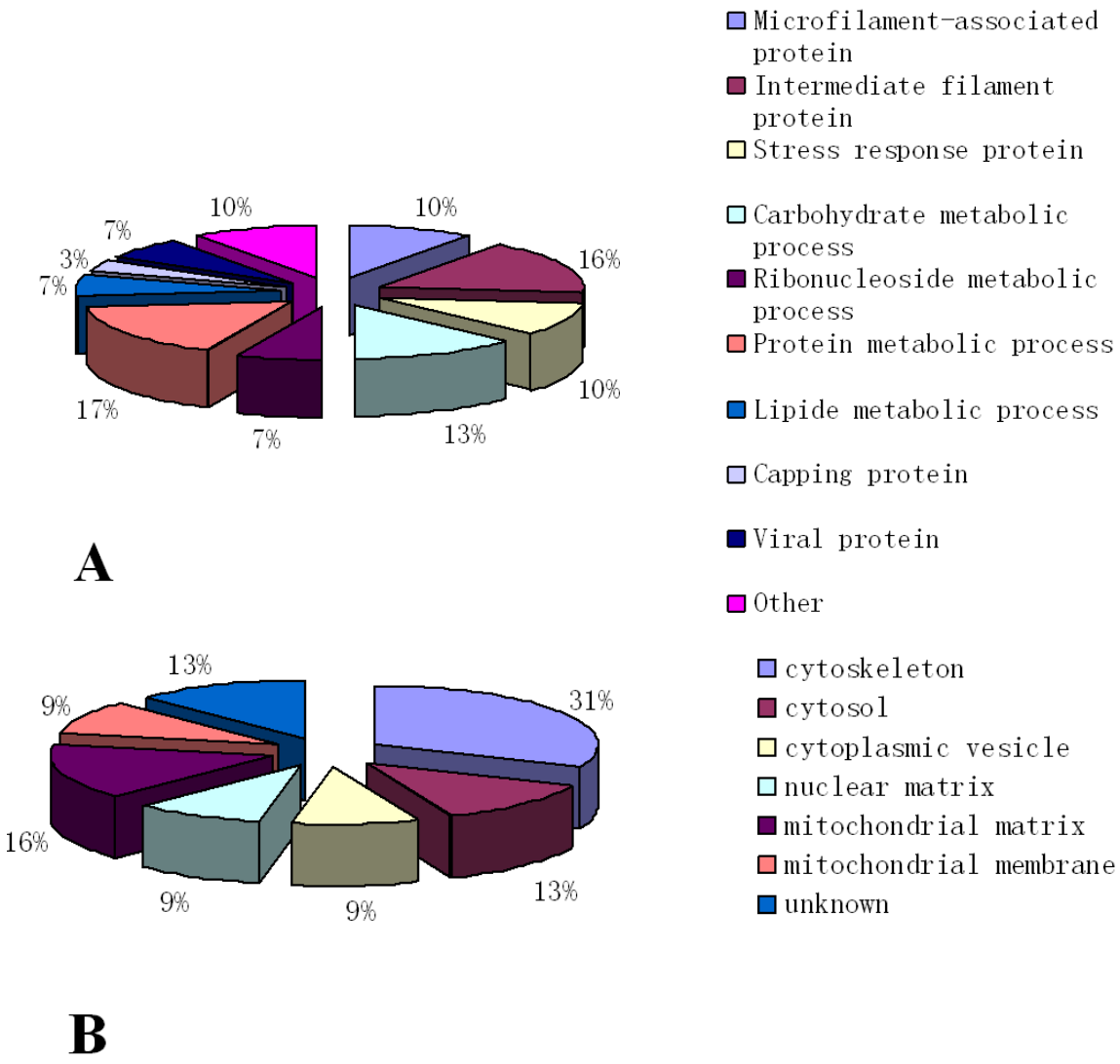

Figure 2. Classification of differentially expressed proteins in FMDV-infected BHK-21 cells, according to the function and subcellular locations of the altered proteins.(A) Functional classification of the affected protein spots. (B) Subcellular location of altered protein spots.

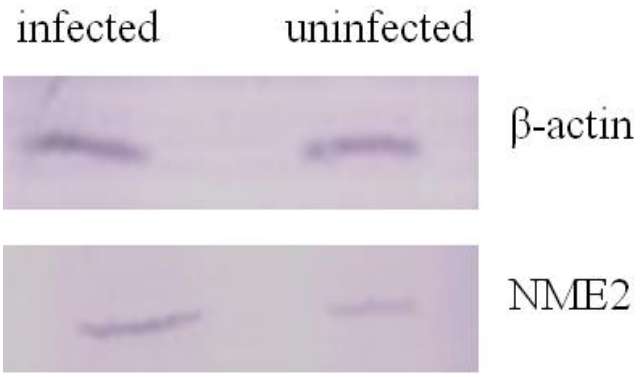

Figure 3. Confirmation of a differentially expressed protein (NME2) in FMDV-infected BHK-21 cells by western blot analysis. β-Actin was used as an internal control to normalize the quantitative data.

often chosen as a simple *in vitro* model for analysis of the direct viral influences on host cell protein machinery, and routinely used for FMDV pathogenic research (Anil et al., 2012; Chen et al., 2004; Huang et al., 2011). Reproduction of FMDV reached plateau period and CPE is the most obvious during 12 h infection. So, the time at 12 h post infection was selected. From the literature, it appears that very few studies have been performed to analyze the interplay between FMDV and host cells using proteomics analysis. In our study, we obtained an overview of the altered protein expression of host cells responding to FMDV infection (Figure 1). The identified cellular proteins function in cytoskeleton organization, metabolic processes proteins, microfilament-associated proteins and stress response proteins (Table 1).

According to the predicted function classification, the

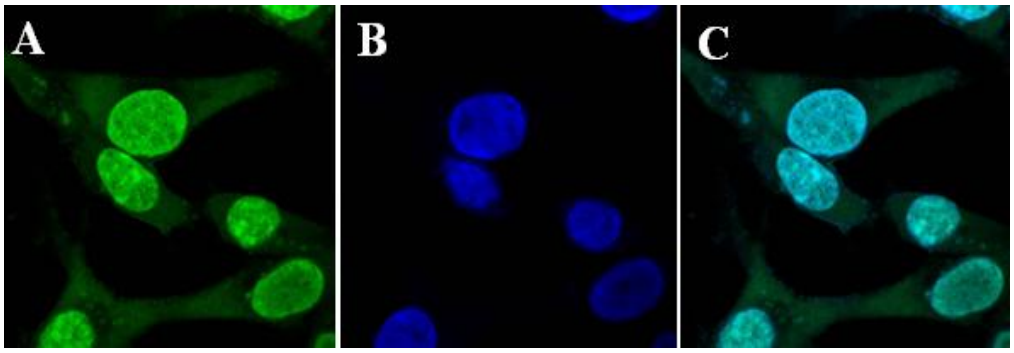

Figure 4. Subcellular distribution of NME2 proteins in BHK-21 cells. (A) Expression of GFP- NME2 fusion protein in the cytoplasm and nucleolus of BHK-21cells. (B) DAPI staining of the nucleolus. (C) A integrated with B.

following proteins accounted for the total differentially expressed proteins: microfilament-associated proteins (10%), intermediate filament protein (16%), stress response proteins (10%), process proteins (44%), capping proteins (3%), FMDV proteins (7%), and other proteins (10%) (Figure 2A). The subcellular localizations of the identified proteins were as follows: cytoskeleton (31%), cytosol (13%), cytoplasmic vesicle (9%), nuclear matrix (9%), mitochondrial matrix (16%), mitochondrial membrane (9%), unknown distribution (13%) (Figure 2B).

The cytoskeletal proteins were the most abundant ones among the significantly altered proteins. These cytoskeletal proteins included capping protein (CP) of actin filament and vimentin. Vimentin is a major component of type III intermediate filaments, which involve cell integrity maintenance, cell movement, cell division process and scaffold structure (Chou et al., 2003). Actin is the major component of microfilaments and essential for a large range of cell functions, including cell division, migration, junction formation, chromatin remodeling, transcriptional regulation, vesicle trafficking and cell shape regulation (Perrin and Ervasti, 2010). We identified two vimentin-related and three actin-related proteins which appeared differentially expressed after infection (Figure 1). These fragments could be products of vimentin and actin cleavage, considering the observed MW and pI (Table 1). Therefore, precise function of vimentin and actin cleavage and specific rearrangement of cell architecture during FMDV infection could be important for better understanding of the FMDV replication process.

Glucose-regulated protein 78 (GRP78) is a stress response protein and a major endoplasmic reticulum (ER) chaperone protein, which is essential for protein quality control in the ER and a central regulator of the unfolded protein response (UPR). The induction of GRP78 is well established as a marker of ER stress (Chen and Lee, 2011). Previous studies have shown that GRP78 is an intracellular antiviral factor against hepatitis B virus (Ma et al., 2009), while GRP78 is also necessary for DENV antigen production and/or accumulation as a chaperone in viral antigen production (Wati et al., 2009). GRP78 expression was upregulated in this study, so we may infer that GRP78 can protect BHK-21 cells from FMDV infection.

Apoptosis is an active process that involves gene activation, expression and regulation (Elmore, 2007; Rasheva and Domingos, 2009). Cellular apoptosis is protective response because it eliminates infected cells (Brereton and Blander, 2010). BHK-21 cells infected with FMDV cause apoptosis, which was confirmed by Bin (2007). In this study, two cell apoptosis-related proteins were identified including PXD1 and NME2. PXD1 is an antioxidant and molecular chaperone that can be secreted by tumor cells (Riddell et al., 2010) and it can catalyze peroxidase reduction of H2O2, organic hydroperoxides and peroxynitrite (Rhee, 2006; Rhee et al., 2005). PXD1 has a role against apoptosis and it is increased and pro- vided enhanced protection against the apoptosis (Berggren et al., 2001). It may have a negative role in ASK1-induced apoptosis (Kim et al., 2008). NME2 is also known as nucleoside diphosphatekinases (NDPK) that are implicated in tumorigenesis as suppressors of tumor metastasis (Leone et al., 1991), it is an isoform of multifunctional proteins involved in a variety of cellular activities including proliferation, development, adhesion and differentiation (Lombardi and Mileo, 2003). As a specific binding protein of Diva and Bcl2L10 and identified as a new biological function, NME2 overexpression induced apoptosis while the depletion led to an increase in Diva's apoptotic activity (Kang et al., 2007). High levels of NME2 could enhance apoptosis in synergy with other metastasis suppressors such as TIP30 (Xiao et al., 2000). Apoptosis is the result of interactions between FMDV and BHK-21 cells. NME2 can promote apoptosis, while PXD1 inhibit apoptosis. In our study, it can be found that NME2 differentially upregulated while PXD1 remarkably down-regulated (Figure 1). It can be concluded that FMDV provide favorable environment for its own replication by regulating NME2 and PXD1 protein expression in BHK-21 cells.

Unexpectedly, we could not detect and identify the other FMDV proteins in our experiment except 2C and P1, the well known cellular substrates of the viral proteinases (e.g., eIF4G) which were not modified in infected cells,

this could be due to the sample preparation method we used and also to the limited resolving power of 2-DE.

This study adopted a gel-based proteomics approach to probe the changed proteins in FMDV infected BHK-21 cells. It is noteworthy that the comparative proteomics approach allowed for the initial identification of 30 altered cellular proteins during FMDV infection and showed that most of the altered cellular proteins appear to have roles in revealing the viral pathogenesis. Clearly, further large scale studies are necessary to understand the roles of the differentially expressed cellular proteins in FMDV infection.

ACKNOWLEDGEMENTS

This work was supported by the National Natural Science Foundation of China (Grant No. 31201914), China Post doctoral Science Foundation funded project (2013M530683) and China Agriculture Research System (CARS-39).The authors wish to thank the journal editors and anonymous reviewers for editing and revising the manuscript

REFERENCES

Aebersold R, Mann M (2003). Mass spectrometry-based proteomics. Nature 422: 198-207.

Alfonso P, Rivera J, Hernaez B, Alonso C, Escribano JM (2004). Identification of cellular proteins modified in response to African swine fever virus infection by proteomics. Proteomics 4:2037-46.

Anil KU, Sreenivasa BP, Mohapatra JK, Hosamani M, Kumar R, Venkataramanan R (2012). Sequence analysis of capsid coding region of foot-and-mouth disease virus type A vaccine strain during serial passages in BHK-21 adherent and suspension cells. Biologicals: J. Int. Assoc. Biol. Stand. 40:426-30.

Bachrach HL (1968). Foot-and-mouth disease. Annual Rev. Microbiol. 22: 201-244.

Berggren MI, Husbeck B, Samulitis B, Baker AF, Gallegos A, Powis G (2001). Thioredoxin peroxidase-1 (peroxiredoxin-1) is increased in thioredoxin-1 transfected cells and results in enhanced protection against apoptosis caused by hydrogen peroxide but not by other agents including dexamethasone, etoposide, and doxorubicin. Arch. Biochem. Biophys. 392:103-9.

Bin LU (2007). Study on the induction of apoptosis in BHK-21 cells by FMDV. Heilongjiang Anim. Sci. Vet. Med. 7: 20-23.

Blackstock WP, Weir MP (1999). Proteomics: quantitative and physical mapping of cellular proteins. Trends Biotechnol. 17:121-127

Brereton CF, Blander JM (2010). Responding to infection and apoptosis-a task for TH17 cells. Ann N Y Acad. Sci. 1209: 56-67.

Chen W, Yan W, Du Q, Fei L, Liu M, Ni Z, Sheng Z, Zheng Z (2004). RNA interference targeting VP1 inhibits foot-and-mouth disease virus replication in BHK-21 cells and suckling mice. J. Virol. 78:6900-7.

Chen WT, Lee AS (2011). Measurement and modification of the expression level of the chaperone protein and signaling regulator GRP78/BiP in mammalian cells. Methods Enzymol. 490, 217-33.

Chou YH, Khuon S, Herrmann H, Goldman RD (2003). Nestin promotes the phosphorylation-dependent disassembly of vimentin intermediate filaments during mitosis. Molecular biology of the cell 14:1468-78.

Elmore S (2007). Apoptosis: a review of programmed cell death. Toxicol. Pathol. 35:495-516.

Hanash S (2003). Disease proteomics. Nature 422, 226-32.

Huang X, Li Y, Fang H, Zheng C (2011). Establishment of persistent infection with foot-and-mouth disease virus in BHK-21 cells. Virol. J. 8:169.

Kang Y, Lee DC, Han J, Yoon S, Won M, Yeom JH, Seong MJ, Ko JJ, Lee KA, Lee, K, Bae J (2007). NM23-H2 involves in negative regulation of Diva and Bcl2L10 in apoptosis signaling. Biochem. Biophys. Res. Commun. 359, 76-82.

Kim SY, Kim TJ, Lee KY (2008). A novel function of peroxiredoxin 1 (Prx-1) in apoptosis signal-regulating kinase 1 (ASK1)-mediated signaling pathway. FEBS Lett. 582:1913-8.

Leforban Y (1999). Prevention measures against foot-and-mouth disease in Europe in recent years. Vaccine 17:1755-1759

Leone A, Flatow U, King CR, Sandeen MA, Margulies IM, Liotta LA, Steeg PS (1991). Reduced tumor incidence, metastatic potential, and cytokine responsiveness of nm23-transfected melanoma cells. Cell 65:25-35.

Lombardi D, Mileo AM (2003). Protein interactions provide new insight into Nm23/nucleoside diphosphate kinase functions. J. Bioenerg. Biomembr. 35: 67-71.

Ma Y, Yu J, Chan HL, Chen YC, Wang H, Chen Y, Chan CY, Go MY, Tsai SN, Ngai SM, To KF, Tong JH, He QY, Sung JJ, Kung HF, Cheng CH, He ML (2009). Glucose-regulated protein 78 is an intracellular antiviral factor against hepatitis B virus. Mol Cell Proteomics 8:2582-94.

Martinez-Salas E, Saiz M, Sobrino F (2008). Foot-and-mouth disease virus. Animal Viruses: Molecular Biology, 1-38.

Maxwell KL, Frappier L (2007). Viral proteomics. Microbiol. Mol. Biol. Rev. MMBR 71:398-411.

Misek DE, Kondo T, Duncan MW (2011). Proteomics-based disease biomarkers. Int. J. Proteomics 894618.

Mitev G, Tekerlekov P (1973). Study of the foot-and-mouth disease virus cultured on the BHK-21 cell line. Veterinarno-meditsinski nauki 10: 3-8.

Perrin BJ, Ervasti JM (2010). The actin gene family: function follows isoform. Cytoskeleton (Hoboken) 67:630-4.

Rasheva VI, Domingos PM (2009). Cellular responses to endoplasmic reticulum stress and apoptosis. Apoptosis 14: 996-1007.

Rhee SG (2006). Cell signaling. H2O2, a necessary evil for cell signaling. Science 312: 1882-3.

Rhee SG, Chae HZ, Kim K (2005). Peroxiredoxins: a historical overview and speculative preview of novel mechanisms and emerging concepts in cell signaling. Free Radic. Biol. Med. 38:1543-52.

Riddell JR, Wang XY, Minderman H, Gollnick SO (2010). Peroxiredoxin 1 stimulates secretion of proinflammatory cytokines by binding to TLR4. J. Immunol. 184: 1022-30.

Rueckert RR (1996). Picornaviridae: the viruses and their replication. Fields Virology 1:609-654.

Schley D, Tanaka RJ, Leungchavaphongse K, Shahrezaei V, Ward J, Grant C, Charleston B, Rhodes CJ (2012). Modelling the influence of foot-and-mouth disease vaccine antigen stability and dose on the bovine immune response. PloS one 7: e30435.

Sun J, Jiang Y, Shi Z, Yan Y, Guo H, He F, Tu C (2008). Proteomic alteration of PK-15 cells after infection by classical swine fever virus. J. Proteome Res. 7:5263-5269

Ubertini B, Nardelli L, Dal Prato A, Panina G, Barei S (1967). BHK 21 cell cultures for the large-scale production of foot-and-mouth disease virus. Zentralblatt fur Veterinarmedizin. Reihe B. J. Vet. Med. Series B.14: 432-41.

Wang H, Wu J, Liu X, He H, Ding F, Yang H, Cheng L, Liu W, Zhong J, Dai Y, Li G, He, C, Yu L, Li J (2012). Identification of short hairpin RNA targeting foot-and-mouth disease virus with transgenic bovine fetal epithelium cells. PloS one 7, e42356.

Wati S, Soo ML, Zilm P, Li P, Paton AW, Burrell CJ, Beard M, Carr JM (2009). Dengue virus infection induces upregulation of GRP78, which acts to chaperone viral antigen production. J. Virol. 83:12871-80.

Wright Jr. GL, Semmes OJ (2003). Proteomics in Health and Disease. J. Biomed. Biotechnol. pp. 215-216.

Xiao H, Palhan V, Yang Y, Roeder RG (2000). TIP30 has an intrinsic kinase activity required for up-regulation of a subset of apoptotic genes. EMBO J. 19:956-63.

Zandi F, Eslami N, Soheili M, Fayaz A, Gholami A, Vaziri B (2009). Proteomics analysis of BHK-21 cells infected with a fixed strain of rabies virus. Proteomics 9: 2399-2407.

Zhang H, Guo X, Ge X, Chen Y, Sun Q, Yang H (2009). Changes in the cellular proteins of pulmonary alveolar macrophage infected with porcine reproductive and respiratory syndrome virus by proteomics analysis. J. Proteome Res. 8:3091-3097.

Zheng X, Hong L, Shi L, Guo J, Sun Z, Zhou J (2008). Proteomics analysis of host cells infected with infectious bursal disease virus. Mol. Cell Proteomics 7:612-25.